IIDEPROQ Scientific Journal
Vol. 3 • 2026

POTENTIAL HYDROGEN PRODUCTION FROM URBAN WASTE BIOGAS VIA SORPTION-ENHANCED STEAM METHANE REFORMING: A MODELING STUDY FOR LA PAZ, BOLIVIA

Pedro Aduviri[1], Lizbeth Echenique[1], Soledad Mamani[1], Yecid Nina[1], Wilfredo Parada[1], Isabel Perez[1], Andres Rojas[1], Cristhian Carrasco[1,*]

ABSTRACT

Using a reproducible mathematical model, the potential for producing hydrogen from methane associated with urban solid waste biogas in La Paz, Bolivia was evaluated. The study integrated two levels: (i) estimation of potential CH_4 generation using LandGEM 3.02 and municipal data on waste transported between 2010 and 2021, and (ii) simulation of a one-dimensional sorption-enhanced steam methane reforming (SE-MSR) reactor with Ni/Al_2O_3 catalyst and *in situ* CO_2 capture via CaO. For LandGEM, $k = 0.04$ year $^{-1}$ y $L_0 = 100$ m^3 CH_4 Mg^{-1} were adopted, values previously used for La Paz and consistent with the *Inventory Conventional* dataset of LandGEM 3.02. The cumulative waste mass for 2010–2021 was 2.505×10^6 Mg. The estimated cumulative generation was 1.538×10^8 m³ of CH_4 by 2039 and 2.068×10^8 m³ by 2059. In the initial state with fresh sorbent, the reactor model predicted 53.74 % CH_4 conversion and a dry H_2 mole fraction of 0.7967, close to the value of approximately 0.80 reported by Neni et al. (2021). The reduced model qualitatively reproduced the coupling between reforming, carbonation, and thermal propagation, but predicted a faster thermal wave than the reference three-dimensional CFD model. Based on the fresh-state yield of 2.133 mol H_2/mol CH_4 fed, methane generation up to 2039 corresponds to a theoretical indicator of 3.280×10^8 m³ of H_2; with an illustrative capture efficiency of 80 %, the indicator decreases to 2.624×10^8 m³. These values represent valorization potential and not industrial production, since they do not include leaks, purification, availability, CaO regeneration, compression, or auxiliary consumption.

Keywords: biogas; hydrogen; LandGEM; steam methane reforming; SE-MSR; CaO; mathematical modeling.

1. INTRODUCTION

Hydrogen is an energy vector and an industrial raw material with high specific energy. However, its environmental performance depends on the production route. Steam methane reforming (SMR) remains a reference technology for producing H_2 from methane, but it generates CO_2 as part of the process chemistry. Integrating a capture stage within the reactor itself, known as sorption-enhanced steam reforming (SE-MSR), shifts the reforming and water-gas shift equilibria by removing CO_2 from the gas phase, with the potential to increase the H_2 fraction in the product (Fernández et al., 2012; Neni et al., 2021; Hu et al., 2023).

Biogas constitutes an alternative source of methane. Its use as reforming feedstock requires prior conditioning to remove species that could affect the catalyst or equipment, such as sulfur compounds, moisture, and other contaminants. Simulation of biogas-fed reformers has shown that the process can be analyzed using non-isothermal one-dimensional models and that behavior depends strongly on the steam/carbon ratio, temperature, pressure, and heat transfer (Chouhan et al., 2021).

[1] IIDEPROQ. Chemical Engineering. Faculty of Engineering. UMSA
***Corresponding author:** ccarrasco@umsa.bo
https://doi.org/10.53287/2026.1q9m5t3h

In Bolivia, the availability and management of urban solid waste varies significantly among municipalities. Available studies show that local characterization and data availability are frequent limitations for evaluating valorization options (Vargas Bautista and Calvimontes, 2017; Ferronato et al., 2021). For La Paz there is a municipal series of waste transported to the Nuevo Jardín de Alpacoma landfill and, subsequently, Sak'a Churu, which allows constant-mass approximations to be replaced with real annual data.

LandGEM 3.02 is an estimation tool based on first-order decomposition kinetics. The model calculates methane generation; it is not directly equivalent to gas captured or available at a plant. Version 3.02 uses a sub-annual integration of 0.1 years, an aspect that is relevant when the degradation constant is high (U.S. EPA, 2005). In this work, the official formulation is used, avoiding the introduction of an external degradable fraction as an independent multiplier of the main equation.

For the SE-MSR reactor, the work of Neni et al. (2021) was taken as a reference; they developed a transient three-dimensional CFD model of a fixed bed with Ni/Al_2O_3 and CaO. Their study reported a maximum dry H_2 mole fraction close to 0.8 while CO_2 capture remained active. The reforming kinetic expressions adopted by Neni et al. derive from the family of equations of Xu and Froment (1989). The reduced model developed here does not aim to reproduce the three-dimensional CFD field, but rather to provide a reproducible, lower-complexity representation for analyzing thermal trends, sorbent consumption, and output performance.

The objective of this work is to evaluate, through reproducible mathematical modeling, the potential for producing hydrogen from methane associated with urban solid waste biogas in La Paz, integrating the estimation of potential CH_4 generation using LandGEM 3.02 with the simulation of a one-dimensional SE-MSR reactor with Ni/Al_2O_3 and CO_2 capture via CaO. The reactor results are contrasted with the behavior reported by Neni et al. (2021), identifying both the trends reproduced by the reduced model and its limitations relative to the reference CFD model.

2. MATERIALS AND METHODS

2.1. General approach

The study was divided into two modules. The first estimated the potential CH_4 generation from urban solid waste using LandGEM 3.02. The second simulated the response of an SE-MSR reactor. The modules were linked solely through a $CH_4 \rightarrow H_2$ conversion indicator; a complete capture, purification, compression, or sorbent regeneration plant was not modeled.

2.2. Methane estimation with LandGEM 3.02

The LandGEM 3.02 equation is expressed as:

$$Q_{CH_4} = \sum_{i=1} \sum_{j=0.1} k\, L_0 \left(\frac{M_i}{10}\right) \exp(-k t_{ij})$$

Where: Q_{CH4} is the methane generation, M is the mass of waste accepted in year i, k is the methane generation rate constant, L_0 is the potential methane generation capacity, and t_{ij} is the age of the j-th fraction of waste in one-tenth of a year (U.S. EPA, 2005).

For the main scenario, k = 0.04 year $^{-1}$ y L_0 = 100 m^3 CH_4 Mg^{-1} were used. These values were used for La Paz by Vargas Bautista and Calvimontes (2017) in the absence of kinetic parameters measured specifically at Bolivian landfills and are consistent with the *Inventory Conventional* dataset of LandGEM 3.02. The annual masses published by the Autonomous Municipal Government of La Paz (2022) for 2010–2021 were used.

The calculated generation was interpreted as potential generation. When an 80 % capture scenario was presented, this value was used only as an illustrative sensitivity and not as a measurement of the landfill studied.

2.3. Reactions considered in the reactor

The reduced model included the three main reforming and shift reactions, in addition to CaO carbonation:

$$CH_4 + H_2O \rightleftharpoons CO + 3H_2 \qquad \Delta H_{298} = 206.2 \text{ kJ MOL}^{-1}$$

$$CH_4 + 2H_2O \rightleftharpoons CO_2 + 4H_2 \qquad \Delta H_{298} = 164.9 \text{ kJ MOL}^{-1}$$

$$CO + H_2O \rightleftharpoons CO_2 + H_2 \qquad \Delta H_{298} = -41.1 \text{ kJ MOL}^{-1}$$

$$CaO + CO_2 \rightleftharpoons CaCO_3 \qquad \Delta H_{298} = -175.7 \text{ kJ MOL}^{-1}$$

The carbon formation and gasification reactions R4–R6 were not included in the main model because the reduced formulation did not incorporate an explicit dynamic state for solid carbon. Their exclusion is treated as a model limitation and not as evidence of the absence of coke.

2.4. Reactor configuration

The geometry and operating conditions were taken from the reference case of Neni et al. (2021). Table 1 summarizes the main parameters.

Table 1. Main reactor and bed parameters

Parameter	Symbol	Value	Unit
Feed temperature	T_{in}	923	K
Pressure	P	35	bar
Steam/carbon ratio	S/C	5	mol/mol
Superficial mass flux	G	3.5	kg m^{-2} s^{-1}
Length	L	7.0	m
Internal diameter	D	0.30	m
Bed porosity	ε	0.50	–
Particle diameter	D_p	0.010	m
Maximum CaO conversion	X_{max}	0.40	–
Effectiveness factor	η	0.30	–
Catalyst bulk density	ρ_{cat}	330	kg m^{-3}
CaO bulk density	ρ_{CaO}	1100	kg m^{-3}
Reported solid density	ρ_s	1675	kg m^{-3}

The source of Neni et al. (2021) presents an ambiguity between the mass description of the bed and some reported volumetric bases. Consequently, the main case was kept conservative with respect to the carbon inventory, and alternative interpretations were retained only as sensitivities.

2.5. Reforming kinetics

Rates R1–R3 were formulated with Xu–Froment-type expressions, adopted from the work of Neni et al. (2021). For partial pressures in bar:

$$R_1 = \frac{k_1}{P_{H_2}^{2.5} DEN^2} \left(P_{CH_4} P_{H_2O} - \frac{P_{H_2}^3 P_{CO}}{K_1} \right)$$

$$R_2 = \frac{k_2}{P_{H_2}^{3.5} DEN^2} \left(P_{CH_4} P_{H_2O}^2 - \frac{P_{H_2}^4 P_{CO_2}}{K_2} \right)$$

$$R_3 = \frac{k_3}{P_{H_2} DEN^2} \left(P_{CO} P_{H_2O} - \frac{P_{H_2} P_{CO_2}}{K_3} \right)$$

Where:

$$DEN = 1 + K_{CO} P_{CO} + K_{H_2} P_{H_2} + K_{CH_4} P_{CH_4} + K_{H_2O} \frac{P_{H_2O}}{P_{H_2}}$$

The kinetic constants were represented using Arrhenius relations:

$$k_i = k_{0,i} \exp\left(- \frac{E_{a,i}}{RT} \right)$$

The complete numerical parameters were kept in the editable supplementary file to avoid duplicating extensive tables in the manuscript.

2.6. CaO carbonation

The evolution of the local sorbent conversion was based on the formulation reported by Neni et al. (2021):

$$\frac{dX}{dt} = k_{carb} (X_{max} - X) (y_{CO_2} - y_{CO_2,eq})$$

with $k_{carb} = 0.35$ s^{-1} y:

$$y_{CO_2,eq} = 4.137 \times 10^7 \exp\left(- \frac{20474}{T} \right)$$

Due to an ambiguity in the placement of the effectiveness factor η between the conversion equation and the published volumetric rate expression, a conservative implementation was adopted in which η is applied only once. In this way, the CO_2 removed from the gas phase remains consistent with the carbon stored as $CaCO_3$.

2.7. Reduced model and numerical solution

The axial domain was discretized with 141 nodes and $\Delta z = 0.05$ m. The gas phase was solved as pseudo-steady-state for each time state of the solid and temperature. The sorbent state $X(z,t)$ and the thermal field evolved transiently. This approximation significantly reduces the computational cost compared with a three-dimensional CFD model, but does not represent radial gradients or complete gas-phase accumulation.

Species conservation in the gas phase was expressed in general form as:

$$\frac{dF_i}{dz} = A_c \sum_r V_{i,r} R_r$$

while the transient energy balance per cell considered the contribution of the reactions, the sensible enthalpy change of the gas, and axial conduction within an effective volumetric thermal capacity. The numerical implementation was verified through carbon balances, spatial and time step sensitivities, integrator tolerances, and specific audits of the pseudo-steady-state approximation.

The main case, called CURRENT_CONSERVATIVE, was run with a numerical partial pressure floor of 10^{-4} bar. The stored long-time run used $\Delta t = 0.1$ s; the time-step sensitivities were not used to recalibrate physical parameters.

2.8. Comparison strategy with Neni et al. (2021)

The comparison with Neni et al. (2021) was treated as a benchmark and not as experimental validation. The following were contrasted: dry H_2 mole fraction, CH_4 conversion, thermal evolution, and propagation of the carbonation zone. The CFD reference reports a maximum outlet temperature of 968.73 K at 615 s and a maximum dry H_2 mole fraction close to 0.8 while capture is active.

2.9. $CH_4 \rightarrow H_2$ potential indicator

To connect both levels of the study, the fresh-state reactor yield was used:

$$Y_{H_2/CH_4} = \frac{n_{H_2,out}}{n_{CH_4,in}}$$

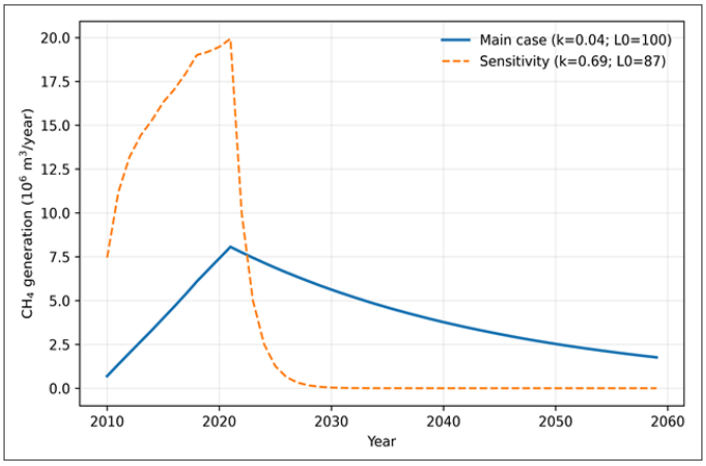
With $n_{H2,out} = 4.97194$ mol s^{-1} y $n_{H4,in} = 2.33134$ mol s^{-1} $Y_{H2/CH4} = 2.13265$ mol/mol. was obtained. Under the same temperature and pressure reference, the molar ratio was used as a volumetric ratio to construct a potential indicator. The stoichiometric limit of four moles of H_2 per mole of CH_4 fed was used only as a theoretical reference.

3. RESULTS AND DISCUSSION

3.1. Potential CH_4 generation via LandGEM

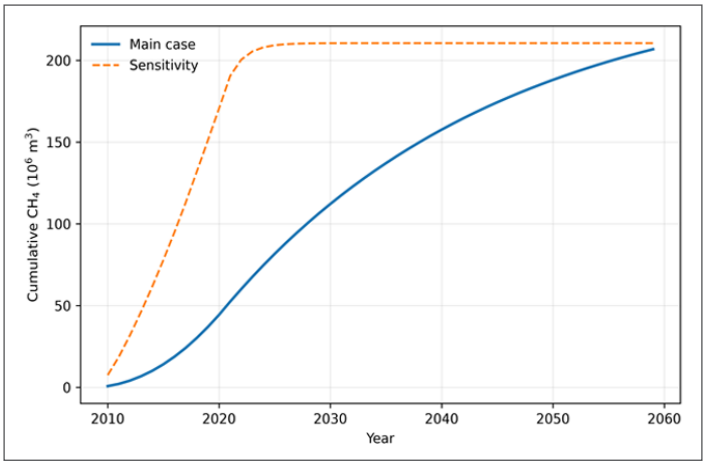
Between 2010 and 2021, 2,504,897 Mg of transported waste were recorded, with an average of 208,741 Mg/year. The series includes Nuevo Jardín de Alpacoma and the subsequent transition to Sak'a Churu, so the geographic scope of the analysis is expressed as the La Paz municipal system and not as the exclusive behavior of a single landfill throughout the entire period.

Figure 1. Annual CH_4 generation via LandGEM



The estimated annual generation reached its maximum in 2021, with 8.064×10^6 m³ CH_4/year, and subsequently decreased according to first-order kinetics. The main scenario produced 153.81 million m³ of cumulative CH_4 by 2039 and 206.77 million m³ by 2059.

Figure 2. Cumulative CH_4 generation



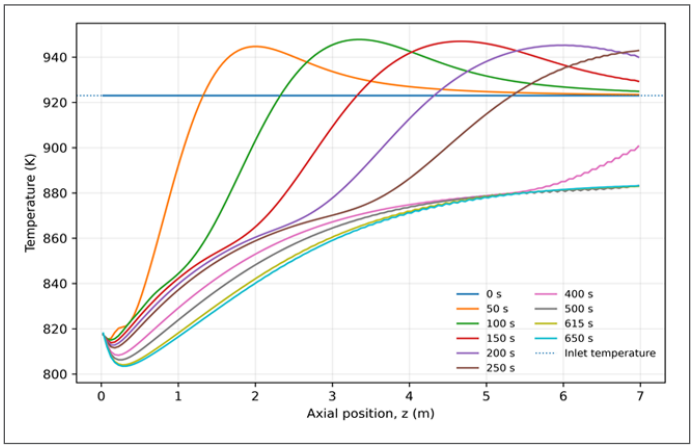
The ultimate capacity associated with the total mass and L_0 = 100 m3/Mg is 250.49 million m³ CH_4. Therefore, by 2059 approximately 82.55 % of this capacity had been generated. The sensitivity scenario with k = 0.69 year^{-1} and L_0 = 87 m3/Mg concentrated the release of CH_4 over much shorter times and produced 36.85 % more cumulative

CH_4 by 2039 than the main scenario. This difference illustrates the model's sensitivity to the selection of k and justifies not treating literature values as locally measured parameters.

3.2. Thermal behavior of the reduced reactor

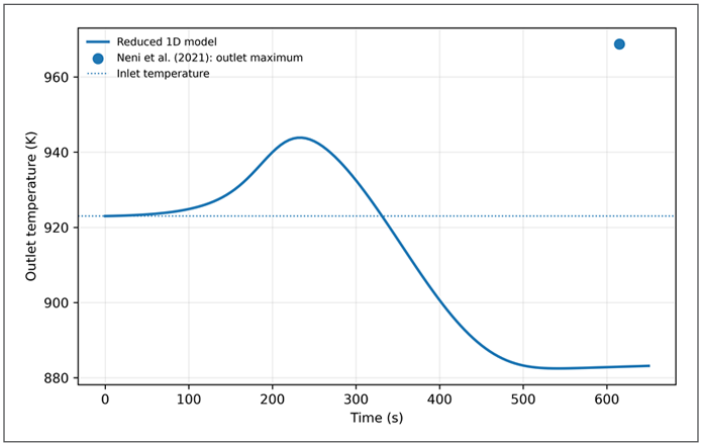
The temperature profiles show the formation and axial propagation of a hot zone associated with the coupling between the endothermic reforming reactions and the exothermic carbonation of CaO.

Figure 3. Axial temperature profiles



In the reduced model, the outlet temperature reached its maximum at approximately 235 s, while Neni et al. (2021) reported 968.73 K at 615 s. At 615 s, the reduced model predicted 882.93 K at the outlet, approximately 85.8 K below the reference CFD maximum.

Figure 4. Outlet temperature of the reduced model and CFD reference point

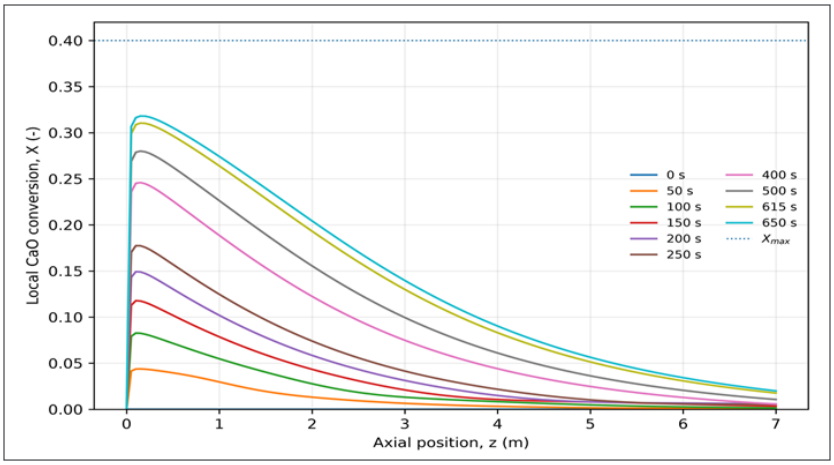


The discrepancy is not interpreted as an isolated numerical error. Sensitivities performed on regularization, spatial step, time step, tolerances, and inventory basis did not eliminate the mismatch. The combination of a faster thermal propagation and a slower sorbent saturation suggests a structural difference between the 1D pseudo-steady-state model and the three-dimensional CFD model, including the representation of transport, the source volumetric bases, and gas-phase accumulation.

3.3. Evolution of CaO carbonation

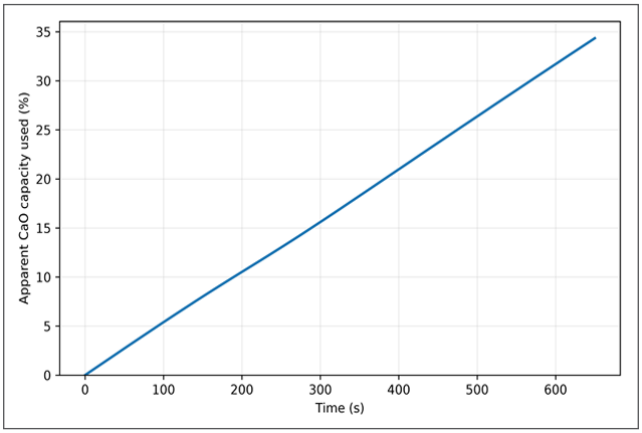
CaO conversion advanced from the inlet toward greater axial positions. Unlike a description based on three time-fixed phases, the results show a continuous evolution that depends on the local availability of CO_2 and on temperature.

Figure 5. Axial profiles of local CaO conversion



The overall indicator of capacity used reached approximately 34.34 % at 650 s. Therefore, the reduced model did not predict complete saturation of the CaO inventory within the simulated horizon.

Figure 6. Use of apparent CaO capacity

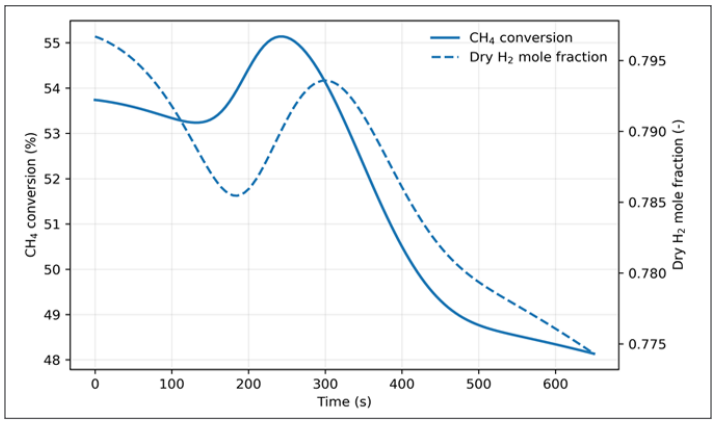


This observation is relevant when comparing with the CFD reference: the reduced model shifts the thermal wave too fast while overall carbonation advances comparatively more slowly. Both differences have opposite signs and cannot be consistently corrected using a single empirical factor without compromising the physical interpretation.

3.4. CH_4 conversion and H_2 production

With fresh sorbent, CH_4 conversion was 53.738 % and the dry H_2 mole fraction was 0.79669. The case without R7 produced approximately 40.84 % CH_4 conversion and 0.6112 dry H_2, which confirms within the model the favorable effect of removing CO_2 from the gas phase.

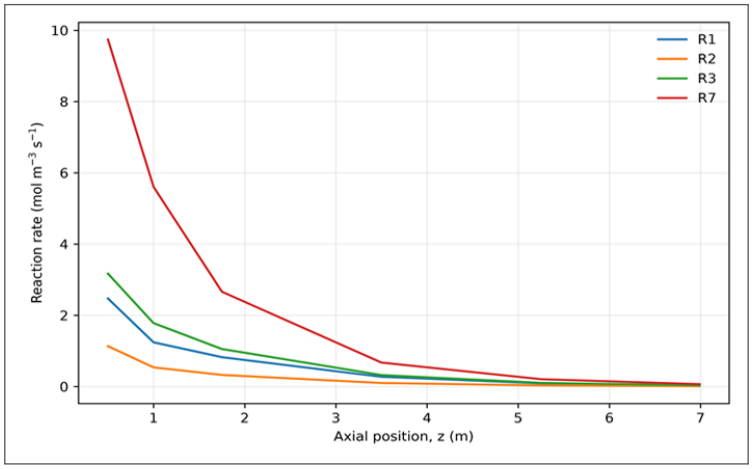
Figure 7. Temporal evolution of CH_4 conversion and dry H_2



The fresh state is very close to the equilibrium calculation at 923 K, 35 bar, and S/C=5, for which 53.93 % CH_4 conversion and 0.79825 dry H_2 were obtained. The dry H_2 fraction of 0.79669 is also close to the maximum value of approximately 0.8 reported by Neni et al. (2021). This closeness constitutes a useful checkpoint, but does not imply validation of the complete transient behavior.

The evolution of local rates shows that the reactions are concentrated mainly in the inlet zone of the reactor in the initial state.

Figure 8. Local rates of R1, R2, R3, and R7 in the initial state



3.5. Synthetic comparison with the CFD benchmark

The results obtained support a moderate conclusion: the 1D model reproduces fundamental qualitative trends of SE-MSR and the increase in H_2 associated with CO_2 capture, but does not quantitatively reproduce the thermal time scale of the CFD of Neni et al. (2021). Therefore, the reference is used as a benchmark to delimit the scope of the reduced model.

Table 2. Comparison of selected indicators

Indicator	Neni et al. (2021)	Reduced model	Interpretation
Dry H_2 mole fraction with capture	≈0.80	0.79669	Good reproduction of the fresh state
Maximum outlet temperature	968.73 K	≈943 K	Lower magnitude in the reduced model
Time of outlet maximum	615 s	≈235 s	Faster thermal propagation
Outlet temperature at 615 s	968.73 K (maximum reported)	882.93 K	Difference ≈−85.8 K

3.6. Indicative valorization potential of CH_4 as H_2

The fresh yield obtained was:

$$Y_{H_2/CH_4} = 2.13265 \text{ mol } H_2 \text{ mol}^{-1} \text{ } CH_4$$

Applied to the CH_4 generated up to 2039, this yield produces an indicator of 328.02 million m³ of H_2. If a methane capture efficiency of 80 % is adopted solely as a scenario, the potentially captured CH_4 would be 123.05 million m³ and the H_2 indicator would decrease to 262.42 million m³.

Figure 9. Indicative bridge from generated CH_4 to H_2

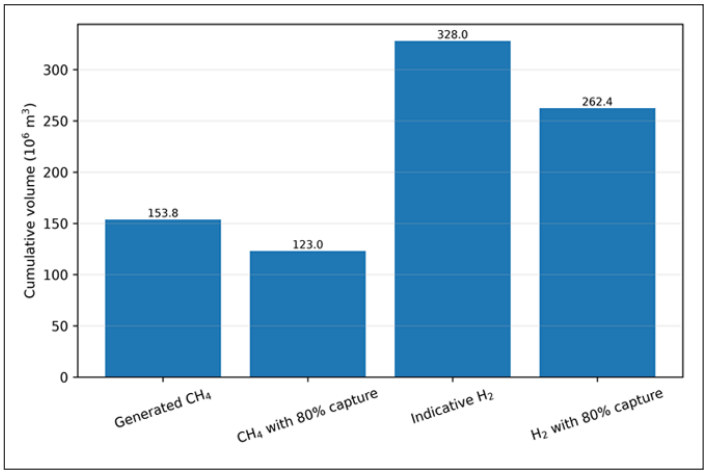


Table 3. Indicative bridge from waste to H_2

Stage	Result
Waste recorded 2010–2021	2.505×10^6 Mg
CH_4 generated up to 2039	153.81×10^6 m³
CH_4 with 80 % capture (scenario)	123.05×10^6 m³
Indicative H_2 without applying capture	328.02×10^6 m³
Indicative H_2 with 80 % capture	262.42×10^6 m³

The indicator does not represent industrial production. Collection losses other than the illustrative scenario, the actual composition and purification of the biogas, plant availability, catalyst deactivation, cyclic sorbent degradation, regeneration energy, compression, H_2 separation, or auxiliary consumption were not considered.

4. LIMITATIONS

The study presents four main limitations. First, the LandGEM parameters used for La Paz come from the literature and not from kinetic measurements specific to the landfill. Second, the 2010–2021 municipal waste series represents transported waste and spans the transition between disposal sites; it does not constitute a complete reconstruction of the entire history of each landfill. Third, the SE-MSR model is a reduced 1D model with a pseudo-steady-state gas phase and does not reproduce the radial transport or the three-dimensional hydrodynamic field of the reference CFD. Fourth, the main model does not incorporate a dynamic solid carbon state or CaO regeneration cycles.

These limitations prevent interpreting the results as a final plant design or as a guaranteed production prediction. The value of the model lies in providing a reproducible, auditable, and coherent calculation chain to relate a potential methane source to the behavior of an SE-MSR reactor under literature conditions.

5. CONCLUSIONS

- The official LandGEM 3.02 formulation, combined with real municipal waste data from La Paz, estimated a cumulative generation of 153.81 million m³ of CH_4 by 2039 and 206.77 million m³ by 2059 for the main scenario with $k = 0.04$ year^{-1} and $L_0 = 100$ m3/Mg^{-1}.

- The reduced SE-MSR model predicted 53.74 % CH_4 conversion with fresh sorbent, and a dry H_2 mole fraction of 0.7967. The comparison with Neni et al. (2021) showed a close reproduction of the initial H_2 level, but a considerably faster thermal propagation: the maximum outlet temperature occurred at around 235 s versus 615 s in the reference CFD.

- The evolution of CaO was continuous and did not reach overall saturation within the 650 s simulated; the capacity used was approximately 34.34 % at the end of the horizon. The combination of an excessively fast thermal wave and a slower saturation indicates that the discrepancy with the CFD is structural and cannot be convincingly attributed to a single numerical parameter.

- The link between LandGEM and the fresh reactor yield produces a theoretical indicator of 328.02 million m³ of H_2 for the methane generated up to 2039, or 262.42 million m³ under an illustrative 80 % capture scenario. These values should be interpreted as valorization potential and not as industrial production.

- Overall, the study shows that urban waste in La Paz represents a potential source of methane suitable for valorization via SE-MSR and provides a reproducible framework for comparing future scenarios with more complete local data and higher-fidelity reactor models.

6. REFERENCES

Chouhan, K., Sinha, S., Kumar, S., & Kumar, S. (2021). Simulation of steam reforming of biogas in an industrial reformer for hydrogen production. *International Journal of Hydrogen Energy,* 46(53), 26809–26824. https://doi.org/10.1016/j.ijhydene.2021.05.152

Fernández, J. R., Abanades, J. C., & Murillo, R. (2012). Modeling of sorption enhanced steam methane reforming in an adiabatic fixed bed reactor. *Chemical Engineering Science,* 84, 1–11. https://doi.org/10.1016/j.ces.2012.07.039

Gobierno Autónomo Municipal de La Paz. (2022). Residuos sólidos transportados a los rellenos sanitarios *"Nuevo Jardín de Alpacoma" y Sak'a Churu,* según mes, 2010–2021. Anuario Estadístico Municipal 2021.

Ferronato, N., Portugal Alarcón, G. P., Guisbert Lizarazu, E. G., & Torretta, V. (2021). Assessment of municipal solid waste collection in Bolivia: Perspectives for avoiding uncontrolled disposal and boosting waste recycling. *Resources, Conservation and Recycling*, 167, Artículo 105234. https://doi.org/10.1016/j.resconrec.2020.10523

Hu, Y., Liu, L., Xu, K., Song, Y., Jing, J., Zhang, H., & Feng, J. (2023). Efficiency analysis of sorption-enhanced method in steam methane reforming process. *Carbon Resources Conversion*, 6(2), 132–141. https://doi.org/10.1016/j.crcon.2022.12.004

Neni, A., Benguerba, Y., Balsamo, M., Erto, A., Ernst, B., & Benachour, D. (2021). Numerical study of sorption-enhanced methane steam reforming over Ni/Al_2O_3 catalyst in a fixed-bed reactor. *International Journal of Heat and Mass Transfer,* 165, 120635. https://doi.org/10.1016/j.ijheatmasstransfer.2020.120635

U.S. Environmental Protection Agency. (2005). *Landfill Gas Emissions Model (LandGEM)* Version 3.02 User's Guide (EPA-600/R-05/047). U.S. EPA Office of Research and Development.

Vargas Bautista, J. P., & Calvimontes, J. (2017). Evaluation of landfill biogas potential in Bolivia to produce electricity. *Investigación & Desarrollo*, 17(1), 55–62. https://doi.org/10.23881/idupbo.017.1-5i

Xu, J., & Froment, G. F. (1989). Methane steam reforming, methanation and water-gas shift: I. Intrinsic kinetics. *AIChE Journal*, 35(1), 88–96. https://doi.org/10.1002/aic.690350109